A. Background Noise

The background noise comes from the fluctuations of the sky's blackbody radiation at around 280 K. The noise equivalent power can be estimated by [13, 14]

$$NEP_{bkgd} = \sqrt{\frac{4\varepsilon h\nu k_B T_B \Delta\nu}{\eta}\left(1+\varepsilon\eta\frac{k_B T_B}{h\nu}\right)} \qquad (5)$$

where ε is the emissivity of the sky, h is Planck's constant, υ is the radiation frequency, k_B is Boltzmann's constant, T_B is the temperature of the background radiation, $\Delta\upsilon$ is the bandwidth of the bandpass filter, and η is the total quantum efficiency of the system. For reasonable weather, with $\varepsilon = 0.5$, $T_B = 280$ K, a quantum efficiency of 10%, we find $NEP_{bkgd} \approx 2\cdot10^{-15}\ W/\sqrt{Hz}$ at 450 μm for a bandwidth of 100 GHz. In actuality, the edges of the atmospheric window are poorer, so a more accurately calculated value is $NEP_{bkgd} \approx 4\cdot10^{-15}\ W/\sqrt{Hz}$.

B. Optical Responsivity

We have measured the optical responsivity of the camera in the laboratory. A room temperature elliptical mirror was mounted on the bottom of the cryostat to reimage the slit inside the cryostat onto an external chopper wheel. The chopper wheel chopped at 10 Hz between 300 K and 77 K sources. For our 450 μm bandpass filter, we expect a chopped signal of 240 pW on each bolometer, estimated using the expression of $2k_B T\left(A\Omega/\lambda^2\right)\Delta\nu$, where A is the area of the bolometer pixel, Ω is the solid angle that the pixel subtends to the aperture stop, λ is the wavelength, and Δυ is the bandwidth of the bandpass filter, which is about 100 GHz for both the 350 μm and the 450 μm filters. At 450 μm, the signal observed on all the pixels is about 2.2 mV peak-to-peak, resulting in an optical responsivity of $9\cdot10^6\ V/W$. Similarly, for the 350 μm filter, the input power at the vacuum window is about 400 pW, and the peak to peak signal is about 4.6 mV, giving an optical responsivity of $1\cdot10^7\ V/W$.

C. Total Quantum Efficiency of the Camera

We have measured the total quantum efficiency of the camera. We record the pixels' I-V curves when we expose the polyethylene window to 300 K and 77 K radiation, respectively. From the zero bias resistance, one can obtain the temperature of the bolometer pixel. Using the thermal conductance G(T) measured earlier, one can estimate the power absorbed by the pixel,

$$P = \int_{T_{sink}}^{T_{bolo}} G(T)dT. \qquad (6)$$

The power absorbed by each pixel with the 450 μm filter in place is 34 pW when the bolometers are exposed to 300 K radiation, and 13 pW when they are exposed to 77 K radiation. Compensating for excess power on the pixel from surrounding walls and some possible small light leaks, the quantum efficiency is estimated using the ratio of the power difference between 300 K and 77 K radiation. This gives a total quantum efficiency in the 450 μm window of about 9%, and 10% in the 350 μm window.

aperture of 46 mm; these filters are made of layers of mylar with a copper mesh pattern deposited on one side of each layer. They are designed with a bandpass width matching the width of the atmospheric windows available from Mauna Kea (altitude 14,000'), the site of the CSO. One selects a filter by turning a shaft from outside the cryostat. We can install four such filters on the filter wheel. Currently a 350 μm and a 450 μm bandpass filter are mounted on the wheel, and the other two positions are used for diagnosing the system.

In addition to the aperture stop and the field stop, we installed radiation baffles to further eliminate light leaks. This is achieved by enclosing the cold imaging optics in a box, as shown in Figure 10. In order to reduce the scattered and reflected radiation from the surfaces of the baffling, the slit, the aperture stop, and the helium radiation shield, we painted them with Z306 Aeroglaze (Lord Corporation Industrial Coatings[11]). We add to the paint, by volume, 3% carbon black and 11% solid glass beads, with a mean diameter of 200 μm (Potters Industries, Inc.[12]). We have tested the reflectivity of this paint on aluminum and copper surfaces using the SIS receivers at the CSO, and found it to be about 35%. With such a configuration of light baffles, the only radiation coming from the vacuum window that can reach the bolometer array is that which passes through the aperture stop and the slit.

It is important to eliminate any radiation from 300 K parts or 130 K FETs. Because the photon energy is high from these sources, even when the photon flux is small, exerting little excess power load on the bolometer, the fluctuation of such a flux can be very large, dominating the NEP of the system. Therefore, in addition to having an enclosed box, we found that it is necessary to baffle around the ^{3}He pot, where there could be direct light passage from the heat switches to the bolometer array, in order to prevent 300 K radiation from the heat switches from reaching the bolometer. Furthermore, we installed baffles around the filter wheel shaft, and put the FETs in light tight housings which are heat sunk to the ^{4}He bath.

6. Characteristics of the Camera

When constructing an instrument for a ground based telescope, the aim is to have the instrument's sensitivity limited by the fluctuation of the background radiation from the sky. For a bolometer instrument, this means that the bolometer's responsivity needs to be high and that the system's electrical noise needs to be low.

Assume that the noise equivalent power from the fluctuation of the background radiation is NEP_{bkgd} $(W/\sqrt{Hz})$, the optical responsivity of the instrument is $\Re$ (V/W), and the voltage noise of the entire system is e_n $(V/\sqrt{Hz})$. The noise equivalent power of the instrument is thus

$$NEP = \frac{e_n}{\Re}. \qquad (4)$$

In order for the instrument to be background limited, the instrument's optical responsivity needs to satisfy $NEP << NEP_{bkgd}$.

atmospheric windows. Undesired radiation from visible wavelengths down to about 170 μm is absorbed by a series of three infrared blocking filters, which are purchased from Infrared Labs[9], and each have about 80% transmission in the passband. On the nitrogen shield is a z-cut quartz wafer anti-reflection coated with black polyethylene on both sides. The helium shield has a z-cut quartz wafer with black polyethylene on one side and a diamond scatter layer on the other, followed by a CsI filter with clear polyethylene antireflection coating on both sides.

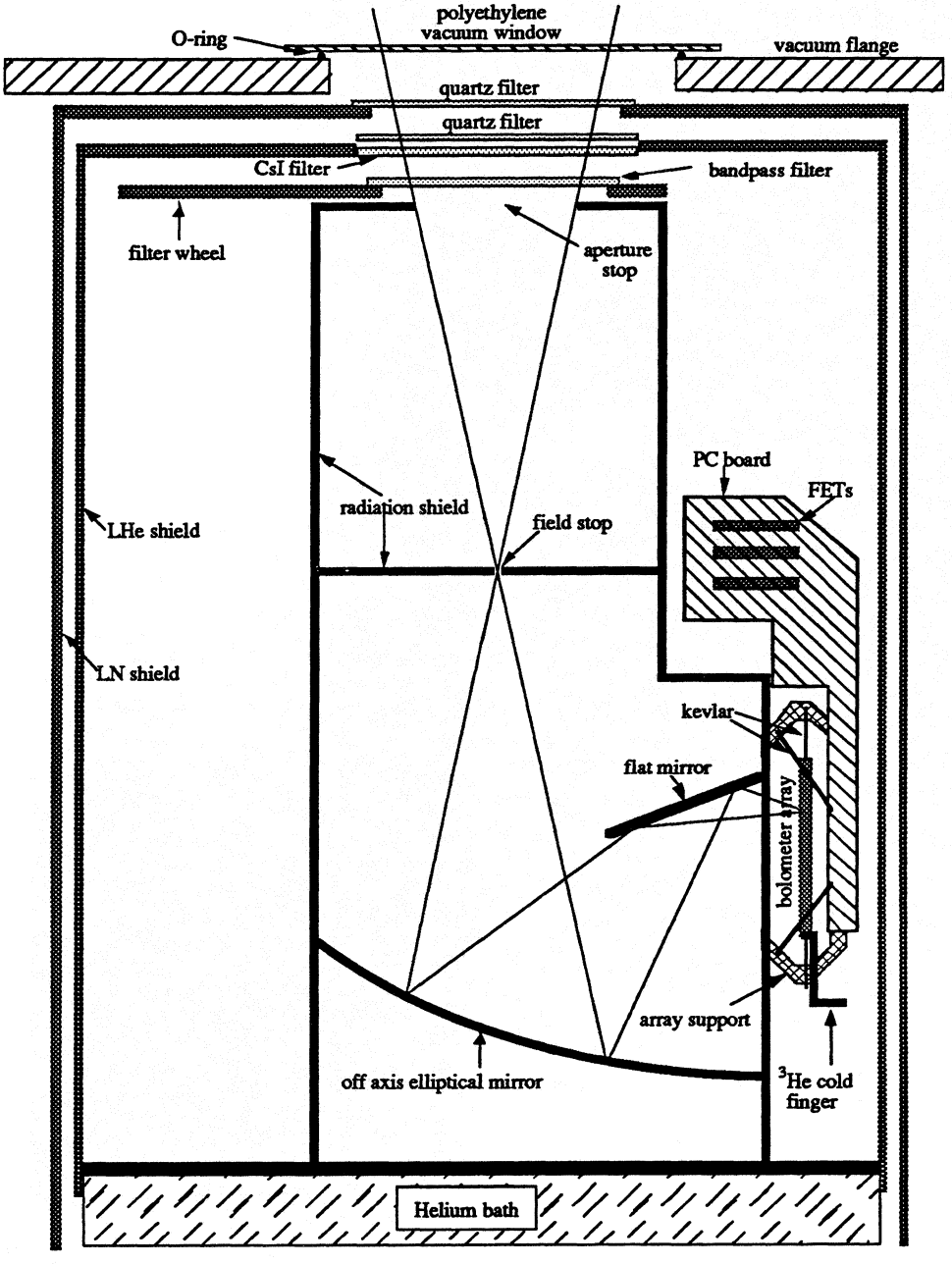

Figure 6. Schematic diagram of the CSO submillimeter high angular resolution camera, 'SHARC'.

The camera is used to observe in the 350 μm and 450 μm atmospheric windows at the CSO. We have purchased 350 μm and 450 μm resonant metal mesh bandpass filters from Cochise Instruments, Inc.[10], with a clear

In order to synchronize the lock-in detection with the chopping secondary, a TTL signal generated by the DSP board is used to synchronize the A/D sampling and to produce the signal that drives the chopping secondary mirror. The chopping frequency can be set to 1 kHz/*n*, where 1 kHz is the A/D sampling frequency and *n* is an integer greater than 1. The A/D, therefore, samples the signal starting at the same place for every chop cycle.

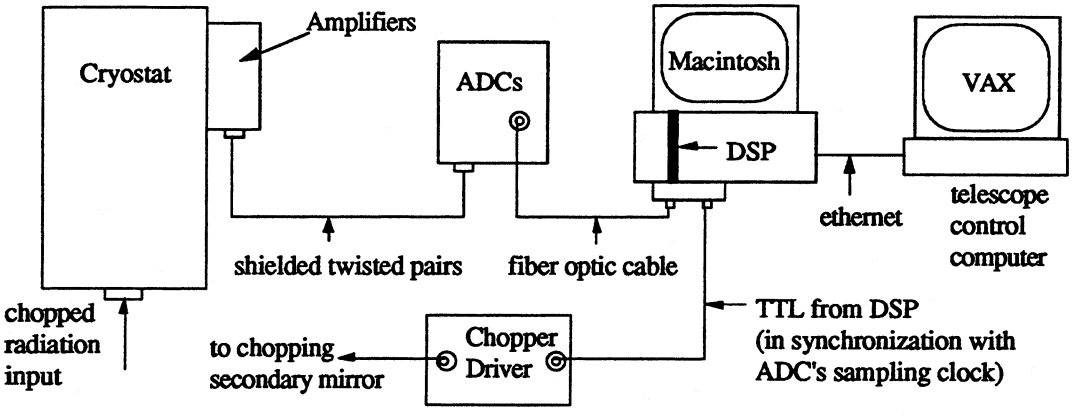

Figure 5. A diagram of the data acquisition system.

5. Cryogenics and Optics Description

A. Cryogenics

Figure 6 shows a schematic of the camera components. The cryostat, with a liquid nitrogen and liquid helium bath, is a single shot ^{3}He refrigerator with a base temperature of 295 mK. A mechanically driven heat switch is employed to control the thermal link between the ^{3}He pot and the ^{4}He bath, and a second one is used between the charcoal pump and the ^{4}He bath. Under normal operation, the ^{4}He bath is pumped with a mechanical pump, and operates at about 1.5 K. The hold time is around 18 hours on the telescope, which limits the continuous operating time of the instrument.

B. Optics Overview

One of the unique features of this instrument is the lack of beam-defining cones, as most recent bolometer systems at $\lambda > 200$ μm have relied on Winston cones. This allows us to use closely packed bolometer pixels to form an array in such a way that we achieve Nyquist sampling of the diffraction pattern at the wavelengths of interest. We use mirrors to focus the light onto the detector pixels, and an aperture stop and a field stop to define the primary illumination and the field of view, respectively.

C. Optical Components

A sheet of 1 mm thick high density polyethylene is used as the vacuum window. We chose polyethylene in order to obtain small deflection under vacuum and good transmission, ~95%, in the 350 μm and 450 μm

Figure 4. This coupler was fabricated on *Duroid* 6010 [9] and is designed to operate at 1.8 GHz. Figure 5 shows the calculated and measured response (s_{21} and s_{24}) of the hybrid.

Fabrication

The primary design parameters used to optimize the mixer performance are the length and impedance of the coplanar transmission lines between the slot antennas and diode bridge. To fabricate the coplanar lines and antennas, a seed layer of chrome/gold is deposited onto a semi-insulating GaAs wafer. Using standard photolithographic techniques, the circuit is defined and the exposed circuit-portion of the seed layer is electroplated with 25 μm of gold. After stripping the photoresist, the unwanted areas of the seed layer are removed with an argon sputter etch followed by a short chrome wet etch. This process leaves the slots, diode mounting pads, and transmission lines patterned on the substrate.

The Schottky diode chips used in the mixer are diced and trimmed to 6 mils $\times$ 2.5 mils so they can be mounted easily onto the circuit. After trimming, the diodes are flip-chip mounted onto the circuit using silver epoxy. Separate IF matching sections were fabricated on *Duroid* 6010 substrates and attached to a lens holder. Coaxial surface mount connectors were soldered to these sections to allow SMA cables from the rat-race hybrid and bias tees to be attached. Using G-wax [10], The mixer chip is mounted to the back of 6 mm diameter silicon hemispherical lens with extension length of 0.5 mm. The complete assembly is then mounted onto the IF matching sections and lens holder. A photograph of the assembled mixer is shown in Figure 6.

Initial Measurements

The test setup used to characterize the mixer is shown in Figure 7. A 50 mW Gunn diode operating at 80 GHz pumps the mixer and is focussed onto the lens assembly through a 2.1 cm diameter teflon lens (focal length of 5 cm). The RF signal was generated with an 80 GHz Gunn

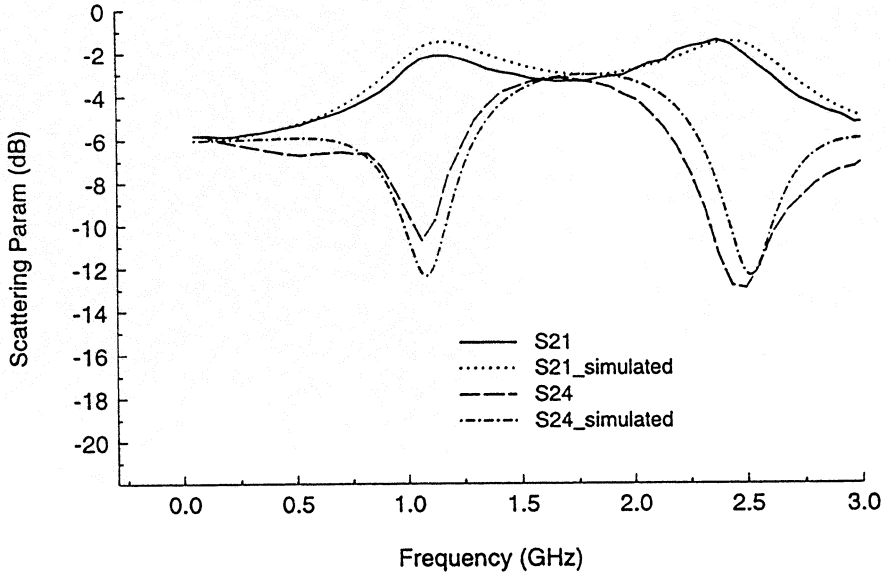

Figure 5. Measured and simulated response of the rat-race hybrid shown in Figure 4.

diode source driving a waveguide doubler. The RF signal is fed to a scalar horn, focused onto the mixer assembly through a second teflon lens (diameter of 5.1 cm and focal length of 7.5 cm), and combined with the LO using a wire grid diplexer.

Circuit simulations with MDS show that 2.5 mW of LO power is sufficient to pump the mixer and give an optimum single sideband (SSB) conversion loss of 6 dB. With the incident LO power estimated to be 2 mW and the incident RF power estimated to be 1 μW, we measure an IF power of -38 dBm, giving a SSB conversion loss of 8 dB. These incident powers were estimated by replacing the mixer assembly with an aperture stop and using a Keating power meter [11] to measure the total power flowing through the aperture. Because of space limitations in our experimental setup, the Keating power meter could not be placed at exactly the same position as the mixer assembly, so these power measurements are approximate. At present, we are reconfiguring our system to accommodate Y-factor measurements using a chopped hot/cold load and plan to characterize the conversion loss and noise temperature of the mixer more fully.

Summary and Future Work

In this paper, we have discussed a quasi-optical mixer that accommodates subharmonic pumping, isolates the RF and LO signals by polarization, and permits DC biasing of the mixer diodes. Initial measurements with an RF signal at 161.8 GHz and LO at 80 GHz indicate the mixer is giving a SSB conversion loss near 8 dB.

The circuit described in this work is designed to be a proof-of-principle demonstration at 160 GHz. However, the mixer configuration is easily scaled to terahertz frequencies with the diodes and circuit monolithically integrated on a single GaAs substrate. After fully characterizing the present circuit, we plan to design and fabricate a subharmonically-pumped double slot mixer based on this topology and operating at 1 THz.

Acknowledgements

The authors are indebted to Dr. G.M. Rebeiz and Dr. D. Filipovic of the University of Michigan for their help in designing the double slot antennas and for providing their computer code for calculating the double slot impedance. We would also like to thank Frank Li and Bill Bishop of the University of Virginia's Semiconductor Device Laboratory for supplying the diodes used in this research and Dave Porterfield for helping with the RF source.

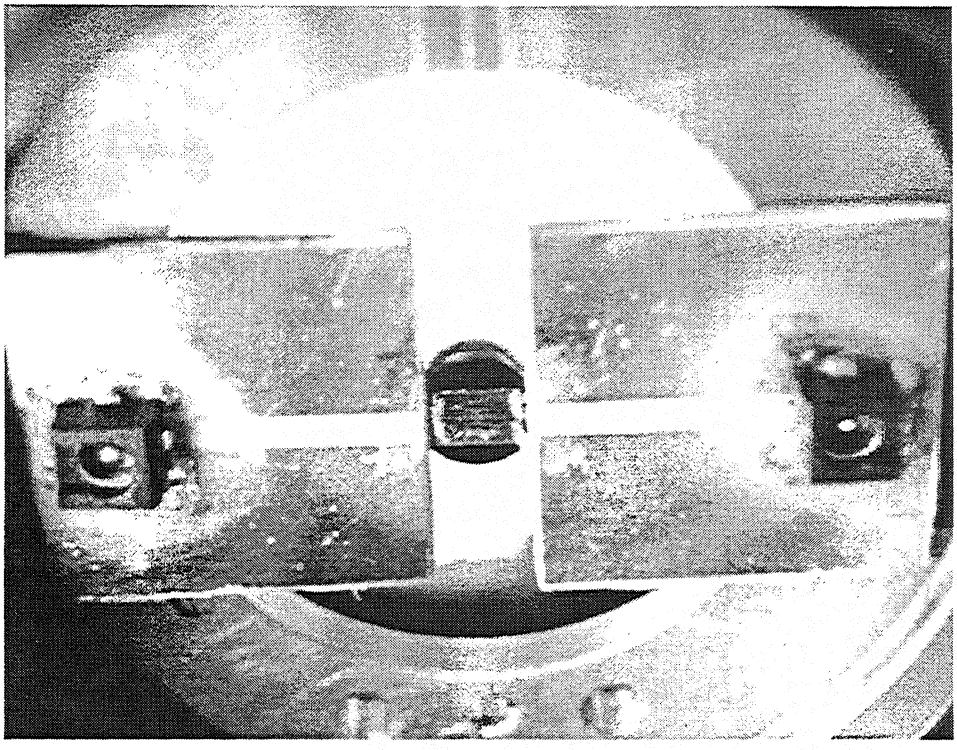

Figure 6. Photograph of the double slot mixer assembly. The mixer circuit is mounted to the back of the silicon hemispherical lens in the center. The IF matching sections and coaxial surface mount connectors are easily seen on each side of the lens.

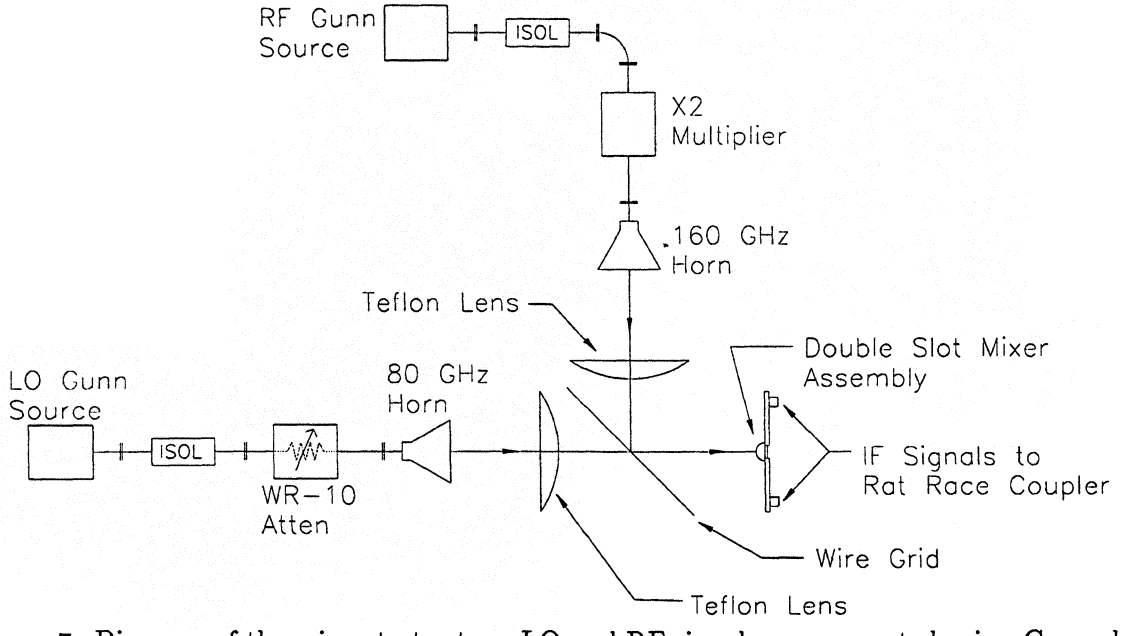

Figure 7. Diagram of the mixer test setup. LO and RF signals are generated using Gunn diode sources and fed to the mixer through scalar feed horns and teflon lenses. A wire grid diplexer is used to combine the LO and RF signals before they illuminate the substrate lens.

REFERENCES

[1] H.P. Röser, E.J. Durwen, R. Wattenbach, G.V. Schultz, "Investigation of a Heterodyne Receiver with Open Structure Mixer at 324 GHz and 693 GHz," *Int'l. Journal of Infrared and Millimeter Waves*, vol. 5, no. 3, pp. 301–313, 1984.

[2] B.K. Kormanyos, P.H. Ostdiek, W.L. Bishop, T.W. Crowe, G.M. Rebeiz, "A Planar Wideband 80–200 GHz Subharmonic Receiver," *IEEE Trans. Microwave Theory Tech.*, vol. 41, no. 10, pp. 1730–1737, October 1993.

[3] S.S. Gearhart, G.M. Rebeiz, "A Monolithic 250 GHz Schottky-Diode Receiver," *IEEE Trans. Microwave Theory Tech.*, vol. 42, no. 12, pp. 2504–2511, December 1994.

[4] S.A. Maas, *Microwave Mixers, second edition*, Artech House, Inc., Boston, 1993.

[5] D.F. Filipovic, S.S. Gearhart, G.M. Rebeiz, "Double Slot Antennas on Extended Hemispherical and Elliptical Silicon Dielectric Lenses," *IEEE Trans. Microwave Theory Tech.*, vol. 41, no. 10, pp. 1738–1749, October 1993.

[6] G.V. Eleftheriades, G.M. Rebeiz, "Self and Mutual Admittance of Slot Antennas on a Dielectric Half-Space," *Int'l. Journal of Infrared and Millimeter Waves*, vol. 14, no. 10, pp. 1925–1946, 1993.

[7] K.K. Rausch, R.F. Bradley, R.M. Weikle, "Finite Element Analysis of a Millimeter-Wave Planar Varactor on Microstrip," *Proceedings of the Int'l Semiconductor Device Research Symposium*, Charlottesville, VA, vol. 1, pp. 393–396, December 1993.

[8] J.L. Hesler, *Planar Schottky Diodes in Submillimeter-Wavelength Waveguide Receivers*, pp. 63–79, Ph.D. Dissertation, University of Virginia, January 1996.

[9] Rogers Corporation, Microwave Materials Division, Box 700, Chandler, AZ 85224.

[10] "G-Wax," Stronghold #7036, Glycol Phthalate Wax, J.H. Young Company, Rochester, N.Y.

[11] Power Meter 103, Thomas Keating, Ltd., Station Mills, Billingshurst, West Sussex, RH14 9SH, United Kingdom.